ELSEVIER

www.elsevier.nl/locate/jelechem

Journal of Electroanalytical Chemistry 472 (1999) 126–136

JOURNAL OF ELECTROANALYTICAL CHEMISTRY

Interaction of H, O and OH with metal surfaces

Marc T.M. Koper *, Rutger A. van Santen

Schuit Institute of Catalysis, Laboratory of Inorganic Chemistry and Catalysis, Eindhoven University of Technology, 5600 MB Eindhoven, The Netherlands

Received 19 March 1999; received in revised form 8 June 1999; accepted 22 June 1999

Abstract

The interaction of the primary water dissociation products H, O and OH with various (111) metal surfaces is studied by density functional theory (DFT) calculations using clusters. It is found that H forms an essentially covalent bond with the metal, whereas O and OH form a largely ionic bond. The O and OH adsorbates prefer the high coordination three-fold hollow site on all metals: no such clear trend for H is found, the adsorption energy for on-top and hollow sites being comparable for most metals, especially on transition metals. The O and OH adsorbates are attracted towards, and donate some electronic charge to the surface when a positive electric field (electrode potential) is applied, whereas the effect of an applied field on H adsorption is much smaller. We also show how the trends in the OH adsorption energies on different metals, as compared with O adsorption, can be explained by a weaker covalent interaction and a stronger Pauli repulsion of the OH with the metal d electrons.

Keywords: Metal surfaces; Water; Dissociation products

1. Introduction

The interaction of water and its dissociation products, i.e. adsorbed H, O and OH, with metal surfaces plays a key role in many electrochemical reactions. Furthermore, the onset potentials of water reduction and oxidation border the so-called double layer region of a certain electrode material. Even though a comprehensive fully quantum mechanical study of the interaction of H_2O, H, O and OH with a metal surface is at present unfeasible, the computational techniques to carry out a combined quantum-chemical and molecular dynamics investigation of water with a metal or semiconductor surface are available and some first simulation attempts have already appeared in the literature [1–4].

Hitherto, most computer simulations of electrified interfaces have either been purely classical, i.e. molecular dynamics simulations of a metal | water interface using interaction potentials derived from quantum-chemical electronic structure calculations [5,6], or have aimed at calculating the adsorption characteristics of specific adsorbates at metal | vacuum interfaces under the influence of an external electric field, thus simulating the electrode polarization (for a review, see Ref. [7]). In the latter type of calculations, the solvent is usually left out of consideration, although some semi-empirical calculations have appeared which include a small number of water molecules [8]. The most accurate method presently available for calculating adsorbate–metal interactions are so-called density functional theory (DFT) calculations based on a periodic supercell slab geometry [9–11]. However, such calculations still require substantial amounts of heavily optimized computer time, especially in the limit of low coverages. The more traditional cluster approach, in which the metal is modeled as a finite cluster of 5 to 50 atoms, remains quite a useful model for obtaining reliable information on the interaction between a single adsorbate and a metal surface in a limited amount of computer time, provided some care is exercised in evaluating the cluster-size effect and the electronic states of the system [12,13].

* Corresponding author. Tel.: +31-40-247-2040; +31-40-245-5054.

E-mail address: m.t.m.koper@tue.nl (M.T.M. Koper)

0022-0728/99/$ - see front matter
PII: S0022-0728(99)00291-0

There have not yet appeared too many ab initio quantum-chemical calculations of the interaction of water and its dissociation products with electrified metal surfaces. In this work, we will employ density functional techniques to study the bonding of water dissociation products (i.e. H, O and OH) at various (111) metal surfaces, in particular Ag(111) and Pt(111), including their electric field dependence. This study is a necessary primer to future work, in which we intend to look at the bonding of water dissociation products with alloy and bimetallic surfaces, which are relevant to electrocatalysis.

2. Computational methods

Cluster models were used to represent the (111) surfaces of the metals considered (for Ru, an hcp metal, our cluster is clipped from the (0001) surface). All clusters, including those containing the adsorbate, possessed C_{3v} symmetry. This means that we consider the OH adsorbate to be oriented in the upright position, with the O closest to the metal plane. Previous studies of the OH adsorption have shown that little energy is gained by allowing the OH to be tilted with respect to the C_{3v} rotational axis [14,15]. We denote a cluster by $M_n(n_1, n_2, n_3)$, where n is the total number of atoms, n_1 is the number of atoms in the first layer, n_2 in the second, and n_3 in the third. The four clusters used are drawn in Fig. 1.

All calculations reported here have been performed using the Amsterdam Density Functional (ADF) Package [16–18]. ADF uses Slater-type orbitals to represent the molecular orbitals. To enhance computational efficiency, the innermost atomic shells of all atoms are kept frozen, as these core electrons do not contribute significantly to the chemical bonding. The extent of these frozen cores was up to and including the following orbitals: Ag 4p, Au 5p, Cu 3p, O 1s, Pt 5p, Ru 4p, Rh 4p, Pd 4p, Ni 3p. All basis sets were of double-ζ quality; in addition the H and O basis sets were augmented by polarization functions. In all cases, the atom–atom distance in the clusters was fixed at the experimental bulk distance [19]. It is known from previous studies that relaxation of the metal surface atoms usually gives only a relatively small contribution to the total adsorption energy [20].

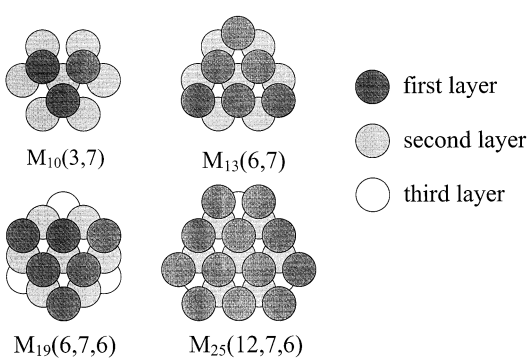

Fig. 1. The four clusters.

The Kohn–Sham one-electron equations were solved in the so-called DFT-GGA approximation [21]. The Vosko–Will–Nusair [22] form of the local density approximation (LDA) was used, and the generalized gradient approximation (GGA) was employed by including self-consistently the Becke and Perdew functionals 'BP86' [23–25] which give non-local gradient corrections for the exchange and correlation parts of the total electronic energy. Such corrections are known to be necessary in order to obtain accurate bonding energies [11]. Relativistic effects within the cores, especially important for the heavier atoms, were accounted for self-consistently by first-order perturbation theory. All cluster calculations were carried out in the spin-restricted mode. The energies of the bare neutral adsorbates however, that we need to calculate the binding energies, were always obtained in the spin-unrestricted mode, since all three adsorbates have an open-shell electronic configuration in vacuum.

The charge on the adsorbates was determined by both the classical Mulliken population analysis and by the Hirshfeld charge analysis [26], in which the adsorbate charge is a weighted spatial integral of the self-consistent field charge density associated with the adsorbate. Orbital analysis was carried out using the DOS utility supplied with the ADF package, which allows the calculation of the total density-of-states (TDOS) of the cluster, the projected or local density-of-states of a particular orbital of the adsorbate (LDOS), and the overlap population density-of-states (OPDOS) or crystal orbital overlap population (COOP), as originally introduced by Hoffmann [27], which enables the calculation of the overlap of a specific orbital on the adsorbate with the sp and d electronic states of the metal cluster. In our OPDOS calculations, the core functions were not included as they do not give a significant contribution to the bonding. Since the finite nature of the clusters in our calculations yields discrete energy levels, the electronic states are artificially broadened by a Lorentzian of half-width σ (usually, $\sigma = 0.5$ eV) to simulate an infinite surface.

3. H, O, and OH interaction with Ag(111)

3.1. Cluster size effect

In Tables 1–3 we report on the binding energies and equilibrium distances for H, O, and OH adsorption at the on-top and hollow (fcc and hcp) sites of Ag clusters of varying size. The last column in Tables 1–3 gives the orbital occupation of the cluster before and after adsorption. In the OH calculations, the O–H distance was

Table 1
Binding characteristics of H on Ag [a]

Cluster	ΔE_b on-top/eV	z_{eq} on-top/Å	
Ag_{10} (7,3)	−1.14	1.70	
Ag_{13} (7,6)	−1.29	1.66	
Cluster	**ΔE_b hollow/eV**	**z_{eq} hollow/Å**	**Orbital occupation before/after adsorption**
Ag_{10} (3,7)	−1.42 (hcp)	0.99	$19e^2/19e^3$
Ag_{13} (6,7)	−1.77 (hcp)	0.96	$15a_1^1/15a_1^2$
Ag_{19} (6,6,7)	−2.01 (fcc)	1.00	$22a_1^1/22a_1^2$
Ag_{25} (12,6,7)	−1.69 (fcc)	1.00	$19a_2^1/19a_2^2$

[a] ΔE_b, the binding energy of the neutral adsorbate; z_{eq}, the distance from the first metal plane. The last column gives valence orbital occupation in the different irreducible representations of the C_{3v} symmetry group before and after the adsorption. Only the changes in occupation are given.

Table 2
Binding characteristics of O on Ag

Cluster	ΔE_b on-top/eV	z_{eq} on-top/Å	
Ag_{10} (7,3)	−1.60	2.03	
Ag_{13} (7,6)	−1.58	2.04	
Cluster	**ΔE_b hollow/eV**	**z_{eq} hollow/Å**	**Orbital occupation before/after adsorption**
Ag_{10} (3,7)	−3.52 (hcp)	1.39	$11a_1^2 19e^2/12a_1^2 20e^2$
Ag_{13} (6,7)	−3.44 (hcp)	1.40	$24e^4 15a_1^1/25e^3 16a_1^2$
Ag_{19} (6,6,7)	−2.79 (fcc)	1.48	$35e^4 22a_1^1/36e^4 23a_1^1$
Ag_{25} (12,6,7)	−2.97 (fcc)	1.43	$27a_1^2 46e^4/28a_1^2 47e^4$

Table 3
Binding characteristics of OH on Ag

Cluster	ΔE_b on-top/eV	z_{eq} on-top/Å	
Ag_{10} (7,3)	−1.36	2.19	
Ag_{13} (7,6)	−1.36	2.22	
Ag_{19} (7,6,6)	−1.00	2.14	
Cluster	**ΔE_b hollow/eV**	**z_{eq} hollow/Å**	**Orbital occupation before/after adsorption**
Ag_{10} (3,7)	−2.26 (hcp)	1.70	$11a_1^2 19e^2/13a_1^2 20e^1$
Ag_{13} (6,7)	−2.52 (hcp)	1.65	$24e^4 15a_1^1/25e^4 16a_1^2$
Ag_{19} (6,6,7)	−2.10 (fcc)	1.64	$35e^4 22a_1^1/36e^4 23a_1^2$
Ag_{25} (12,6,7)	−2.03 (fcc)	1.68	$27a_1^2 46e^4 19a_2^1/18a_2^2 29a_1^2 47e^4$

fixed at its computed equilibrium length in vacuum, 0.9958 Å. It is observed that all three adsorbates prefer the high-coordination sites. The equilibrium distances, z_{eq}, defined as the distance from the first metal plane, do not vary much with the cluster size. The binding energy, however, shows some considerable fluctuation with cluster size. For simple adsorbates, these fluctuations may be understood and partly removed by the bond preparation ideas put forward by the Siegbahn group [12,28,29]. The bond preparation scheme generally depends on the adsorbate and its type of bonding.

For H adsorption, the bond preparation rule is simple and requires that the bare metal cluster has an open-shell character with a single electron in the highest occupied orbital of s symmetry, i.e. an a_1 orbital, in order to form a covalent bond with a singly-occupied 1s orbital on the hydrogen [12,28]. Not all ground states conform to this bond-prepared state, and hence it is preferable to calculate the binding energy with respect to the state in which an electron from the HOMO orbital is excited to the lowest-lying empty a_1 orbital. For a real metal, this excitation energy is virtually zero,

but for a cluster it may amount to several tenths of an eV. It is seen that for the clusters in Table 1, the Ag_{13} and Ag_{19} clusters satisfy the bond preparation rule, as the H 1s electron has combined with a singly occupied a_1 electron of the bare metal cluster (see last column of Table 1). The Ag_{10} ground state is not bond prepared and hence the bond energy predicted for this cluster, when referred to the ground state, is too small. However, exciting the system to occupy the lowest-lying a_1 orbital overshoots the bond energies found for the Ag_{13} and Ag_{19} clusters due to the larger HOMO–LUMO gap for the small cluster. This 'overshooting' was also mentioned by Panas et al. [28] in their study of H adsorption on Ni(111) clusters. For the Ag_{25} cluster we find quite a similar overshooting of the bonding energy. Apparently, one needs quite a high density-of-states near the Fermi level for the bond preparation concept to give quantitatively good adsorption energies. A transition metal such as Ni is therefore better adapted to apply bond preparation rules than Ag which lacks a significant contribution from the dense d-orbitals near the Fermi level. Nevertheless, we believe that a value of 1.8 to 2.0 eV should be quite a reliable value for the bond energy of H at the hollow site of Ag(111). Our results also seem to indicate that the 'unfilled' fcc site is slightly preferred over the filled hcp site for H adsorption.

In the case of O adsorption, Siegbahn and Wahlgren [29] have studied the bonding mechanism on Ni(100) and Ni(111) clusters and found no single bonding mechanism as for H adsorption. Various electronic states of the cluster may be prepared for bonding. It can be seen from the calculation results that most typically two electrons from the O occupy an a_1 orbital of the cluster and the other four occupy an e orbital. This bonding mechanism is 'mechanism 1' of Siegbahn and Wahlgren, who also found this to be the most dominant bonding type. In contrast to H adsorption, O adsorption seems to prefer the filled hcp site.

In the case of OH adsorption, Hermann et al. [30] found that for OH on Cu the bond is created by charge transfer from the Cu cluster to the OH forming an OH^- closed shell configuration ($3a_1^2 1e^4$ in the C_{3v} symmetry). The transfer is most easily accomplished if the highest occupied orbital of the bare metal cluster is of A_1 or E symmetry. For Ag, we find a similar bonding mechanism, as the bonding turns out to be essentially ionic (see Section 3.2). Of the four clusters in Table 3, only the Ag_{25} cluster is not bond prepared as the HOMO level of the metal cluster is an orbital of A_2 symmetry. Note that it is exactly this cluster that gives the lowest bonding energy. As for O chemisorption, the preferred binding site for OH on Ag seems to be the filled hcp site.

3.2. Analysis of the bond and its electric field dependence

In this section, we will have a closer look at the binding characteristics of the H, O, and OH adsorbates in their most stable adsorption site, the three-fold hol-

Table 4
Binding characteristics of H in the hcp hollow site on Ag_{13} for three different electric fields [a]

Field/a.u.	ΔE_b/eV	ΔE_b^{st}	ΔE_b^{orb} (A_1)	ΔE_b^{orb} (E)	z_{eq}/Å	q_H M/H
−0.01	−1.89	4.37	−6.38	0.11	0.98	−0.23/−0.14
0	−1.77	4.33	−6.25	0.16	0.96	−0.22/−0.12
0.01	−1.63	4.27	−6.09	0.20	0.94	−0.20/−0.10

[a] q_H M/H is the adsorbate (H) charge according to the Mulliken (M)/Hirshfeld (H) analyses.

Table 5
Binding characteristics of O in the hcp hollow site on Ag_{13} for three different electric fields

Field/a.u.	ΔE_b/eV	ΔE_b^{st}	ΔE_b^{orb} (A_1)	ΔE_b^{orb} (E)	z_{eq}/Å	q_O M/H
−0.01	−3.77	5.40	−2.01	−7.19	1.47	−0.71/−0.42
0	−3.44	5.99	−2.46	−6.98	1.40	−0.70/−0.37
0.01	−3.11	5.93	−2.66	−6.37	1.39	−0.66/−0.32

Table 6
Binding characteristics of OH in the hcp hollow site on Ag_{13} for three different electric fields

Field/a.u.	ΔE_b/eV	ΔE_b^{st}	ΔE_b^{orb} (A_1)	ΔE_b^{orb} (E)	z_{eq}/Å	q_O M/H	q_{OH} M/H
−0.01	−2.58	3.72	4.77	−10.99	1.71	−0.67/−0.40	−0.42/−0.34
0	−2.55	4.05	3.03	−9.40	1.65	−0.68/−0.36	−0.37/−0.27
0.01	−2.57	4.12	1.26	−7.85	1.62	−0.68/−0.35	−0.33/−0.20

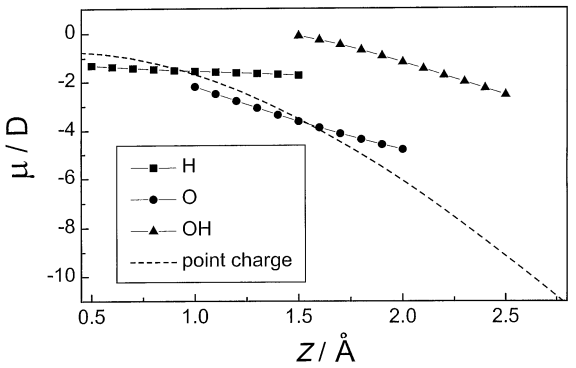

Fig. 2. The dipole moment curves of H, O, and OH interacting with the Ag_{13} cluster. Also shown as a dashed line is the dipole moment curve of a -1 point charge interacting with a Ag_{13}^{+} cluster. $1D = 3.33 \times 10^{-30}$ C m.

low, at the Ag_{13} cluster, for a positive, zero and negative applied field. Results of the binding characteristics are given in Tables 4–6.

First, we want to establish the dominant bonding mode, covalent or ionic, for the three adsorbates. The Mulliken and Hirshfeld charges found for zero field suggest that while H forms an essentially covalent bond, O and OH carry a relatively high negative charge and hence form an ionic bond. A convenient tool to study the bond ionicity further is to plot the cluster dipole moment as a function of the distance between the metal cluster and the adsorbate [31]. This plot is given in Fig. 2, for the three adsorbates and a -1 point charge interacting with the Ag_{13}^{+} cluster. In agreement with the Mulliken and Hirshfeld charges, the dipole moment curves indicate that H forms a covalent bond, whereas O and OH form a largely ionic bond. Since for both OH and O the dipole moment curves are less steep than the point charge curve, our calculations indicate that OH and O carry a partial negative charge which is less than a full electronic charge.

A third way to assess the bonding type is to study the character of the bond as a function of an applied electric field [31]. This is also a convenient, though perhaps rough, way to model the influence of changing the applied electrode potential in an electrochemistry experiment. Even though the electronic polarization within the cluster may be different from that of an extended surface, the field models two important aspects of the electrode potential: the relative shift of the metal electronic levels with respect to the adsorbate levels, and the presence of an electric field at the location of the adsorbate. This gives us some confidence that the trends found with the electric field should be very similar to that of a 'real' electrode potential. An applied field of 0.01 a.u. corresponds to ca. 0.52 V $Å^{-1}$, and hence to a change in applied potential of roughly 1 to 2 V. There seems to be some ambiguity in how to define the bonding energy in the case of an applied field, and we have chosen to adhere as closely as possible to the electrochemical situation in that the bonding energy of the adsorbate X at a certain value of the field F is given by $\Delta E_b(M-X;\ F) = E(M-X;F) - E(M;F) - E(X;0)$, that is: we refer the bonding energy at field F to the energy of the cluster at field F and the energy of the isolated adsorbate under field-free conditions $F=0$, since in an electrochemistry experiment the electric field in the bulk of the electrolyte solution either vanishes (when no current flows) or is very small. In our definition of the field, a positive field corresponds to a more positive electrode potential, as electrons are attracted to the metal surface. This is clearly seen in the field dependence of the Mulliken and Hirshfeld charges of the three adsorbates, as with a more positive applied electric field electrons flow from the adsorbate to the metal.

When looking at the bonding energy as a function of the applied field, it is interesting to see how the various contributions such as steric and orbital interactions vary in making up the total bonding energy [32]. ADF allows a subdivision of the total bonding energy into two main contributions: a steric bonding energy (ΔE_b^{st}) which is commonly defined as the energy difference between the separate fragments and the composite system, where the latter is described by the determinantal wave function which is the antisymmetrized product of overlapping fragment orbitals. No electron relaxation due to the formation of bonds is accounted for, only the rise in kinetic energy due to the orthogonalization of the fragment orbitals. The steric repulsion consists of an attractive electrostatic part and a repulsive Pauli contribution, and since the latter dominates, the steric repulsion energy is a positive quantity. The difference between the total bonding energy and the steric repulsion is due to the orbital interactions (ΔE_b^{orb}), and these can be subdivided into the contributions of the orbitals with different symmetry. As expected, for all three adsorbates we find significant orbital interaction contributions only from orbitals with A_1 or E symmetry. The three contributions, ΔE_b^{st}, ΔE_b^{orb} (A_1) and ΔE_b^{orb} (E) are given in Tables 4–6 as a function of the applied electric field.

For H, we find that the influence of the electric field is rather small. Both the bonding energy, the equilibrium bond distance and the adsorbate charge are not strongly dependent on the field. This corroborates our earlier conclusion that the bond is essentially covalent. Also, note that the orbital interaction energy is essentially only of A_1 character, in agreement with the bond preparation concepts in the previous section.

For O chemisorption, there is a stronger influence of the electric field. With a more positive field, the O adsorbate is pulled towards the surface, which again suggests that adsorbed oxygen is an essentially negatively charged adsorbate. However, the bond energy (in our

Table 7
Binding characteristics of H in the hcp hollow site and the on-top site of M_{13} clusters [a]

M	ΔE_b/eV hollow	z_{eq}/Å	q_H (H)	q_H (M)	E_b/eV on-top	z_{eq}/Å	q_H (M)	q_H (H)
Ag	−1.77	0.96	−0.22	−0.12	−1.29	1.66	−0.21	−0.12
Au	−1.88	0.84	−0.65	−0.08	−2.08	1.56	−0.53	−0.03
Cu	−2.23	0.90	−0.07	−0.14	−1.54	1.52	0.02	−0.13
Pt	−2.61	1.03	−0.35	−0.08	−3.11	1.56	−0.30	−0.05
Ru	−2.63	1.12	−0.24	−0.11	−2.67	1.63	−0.11	−0.08
Rh	−2.08	1.00	−0.10	−0.07	−2.69	1.55	−0.04	−0.07
Pd	−2.76	0.92	−0.18	−0.07	−2.57	1.53	−0.11	−0.08

[a] q_H (H/M) is the charge on the adsorbate according to the Mulliken/Hirshfeld analyses.

definition) becomes lower, due to increased steric repulsion and the less attractive *e* orbital interactions. The orbital interactions clearly depend on the difference in occupation of the various orbitals between the bare metal cluster and the metal–adsorbate cluster, and in fact in this sense the Ag_{13}–O cluster is not typical as three O electrons occupy a_1 cluster orbitals and three O electrons occupy *e* cluster orbitals, whereas for the other clusters this is two and four, respectively (see Table 2). However, as we checked for the Ag_{10}–O cluster, the trends in dependence on the applied field remained the same: the a_1 orbital interaction gets more negative with a more positive applied electric field (though for the Ag_{10} cluster it is repulsive, in the absolute sense), whereas the *e* orbital interaction gets weaker with a more positive applied electric field. The total bonding energy gets lower for more positive electric fields, both for the Ag_{10} and Ag_{13} clusters.

In our calculations, the binding energy of OH is not field dependent (Table 6). As for O, the OH adsorbate is pulled towards the surface with a more positive field, implying a negatively charged adsorbate, but, unlike O, the changes in the steric and orbital interactions cancel each other out.

It is important to realize that a decreasing oxygen interaction with a more positive field, i.e. with a more positive electrode potential, does not mean that the discharge of water into adsorbed oxygen becomes thermodynamically less favorable with increasingly positive electrode potential. This would clearly be in contradiction with experimental experience. In an electrochemistry experiment, the real reaction is:

$$H_2O \rightarrow O_{ads} + 2H^+ + 2e^-$$

Even though the intrinsic interaction of oxygen with a metal surface may become somewhat weaker with positive potential (at least according to our calculations on Ag and our definition of the adsorption energy in the presence of an electric field) the electrons liberated are stored at a lower Fermi level. which is thermodynamically favorable. If a field of 0.01 a.u. were to correspond to a change in the voltage drop across the double layer of ca. 2 V, the ca. 0.3 eV loss in adsorption energy of oxygen would be completely outweighed by the ca. 4 eV lowering in the energy of the electrons.

4. H, O, and OH interaction with other metals

4.1. Binding energies

In Tables 7–9 we report the adsorption energies of the three adsorbates on six different metals, three noble coinage metals Ag, Au and Cu, and three transition metals Pt, Ru and Rh. For all coinage metals, the adsorption energies were calculated with respect to the ground-state bare metal cluster, as we found that a bond-prepared cluster may quite seriously overshoot the adsorption energy, especially if the density-of-states near the Fermi level is relatively low as is the case with the Ag, Au and Cu clusters. The adsorption energies

Table 8
Binding characteristics of O in the hcp hollow site of M_{13} clusters

M	ΔE_b/eV	z_{eq}/Å	q_O (M)	q_O (H)
Ag	−3.44	1.40	−0.70	−0.37
Au	−2.69	1.50	−0.60	−0.29
Cu	−4.72	1.23	−0.75	−0.38
Pt	−3.75	1.46	−0.62	−0.26
Ru	−5.08	1.38	−0.70	−0.28
Rh	−4.67	1.33	−0.68	−0.23

Table 9
Binding characteristics of OH in the hcp hollow site of M_{13} clusters

M	ΔE_b/eV	z_{eq}/Å	q_{OH} (M)	q_{OH} (H)
Ag	−2.55	1.65	−0.37	−0.27
Au	−1.80	1.80	−0.30	−0.24
Cu	−3.01	1.48	−0.37	−0.23
Pt	−2.38	1.65	−0.37	−0.27
Ru	−2.69	1.68	−0.32	−0.15
Rh	−2.75	1.68	−0.30	−0.13
Ni	−2.86	1.46	−0.37	−0.20

agree quite well with the slab calculations of Hammer and Norskøv [20] (see below) and with experiment [33], and therefore we believe that the reported values should be quite reliable.

For the O and OH adsorbates, we find the hollow site to be preferred to the on-top site. Oxygen adsorption is usually about 1.5 to 2 eV, and hydroxyl adsorption about 1 eV stronger in the hollow site. Remarkably, according to our calculations there does not seem to be a uniquely preferred coordination for H adsorption. Therefore, we give in Table 7 the adsorption energies for both three-fold and on-top sites. We find that the difference between on-top and three-fold hollow sites is quite small for Au and all transition metals (the on-top site is even preferred for Au, Pt and Rh). We have also included Pd in the Table, as detailed periodic supercell slab calculations are available for this metal [34]. These calculations, which assume finite coverages, find that the fcc and hcp three-fold hollow sites are more stable than the on-top site by ca. 0.4 and 0.3 eV, respectively, for H coverages of 1 and 1/3. In fact, Pd is the only transition metal for which we also find the (hcp) hollow site to be significantly more stable than the on-top site, by ca. 0.2 eV. Clearly, our calculations may suffer from the cluster effect (the Pt on-top and Rh hcp hollow results could result from some cluster artifact, even though they were bond prepared) but are free from any lateral interaction effects. It seems that this matter deserves further attention in the future, certainly if one realizes that the H coordination to transition metal electrodes in the underpotential region is still a matter of disagreement in the recent literature. Jerkiewicz has claimed that the adsorption energy for H in the underpotential region on Pt and Rh, ca. 240 to 260 kJ mol^{-1} = ca. 2.5 to 2.7 eV, implies that H is adsorbed in the hollow site [35]. Our results indicate that it can be deceptive to deduce the type of adsorption site for hydrogen on transition metals from the experimentally obtained adsorption energy.

Of the coinage metals Ag, Au and Cu, Cu is the most hydro- and oxophilic, i.e. the least noble. The energies found, generally agree well with other theoretical values from the literature provided these studies included gradient corrections. For instance, Hammer and Norskøv [20] report for a p(2 × 2) overlayer on (111) surfaces using DFT-GGA calculations on a slab geometry, H binding energies of ca. −2.1 and −2.4 eV for Au and Cu, and O binding energies of −3.2, −2.6 and −4.5 eV on Ag, Au and Cu. For OH adsorption on a Cu cluster, Hermann et al. [30] reported a SCF-CI binding energy of ca. −3.0 eV, agreeing very well with our value. The O adsorption energies were calculated assuming the bonding mechanisms as described in the previous section, with either 2 or 3 O electrons occupying cluster orbitals of A_1 symmetry, and 4 or 3 O electrons occupying cluster orbitals of E symmetry, respectively. None of the ground-state bare transition metal clusters possessed a HOMO level of A_2 symmetry and so they were all bond prepared for OH. Pt generally shows the lowest affinity for the water dissociation products, and Ru the highest in agreement with the slab calculations of Hammer and Norskøv.

The calculated adsorption energies generally agree quite well with experimental values [33]. For H adsorption on transition metals, the bonding energy is reported to be -60 kcal $mol^{-1} \approx -2.60$ eV, whereas on the coinage metals it is typically 0.4 to 0.5 eV weaker. The O adsorption energies on Ag and Pt compare favorably with the experimental values, −3.33 and −3.69 eV, respectively. Oxygen is found to adsorb more strongly on Rh and Ru than on Pt, though the experimental adsorption energies are not as negative as calculated.

4.2. Density-of-states analysis of H, O, and OH adsorption

It is quite natural to presume that the differences between the bonding of adsorbates on coinage and transition metals is at least partly explained by the different roles played by the d-band in the two groups of metals. For the coinage metals, the d-band is completely filled and relatively far below the Fermi level; for the transition metals, the Fermi level lies within the only partially filled d-band. Several authors have attempted to understand trends in adsorption characteristics such as bonding energies, LDOS, and OPDOS by a simple Anderson–Newns-type modeling in which the metal was characterized by a broad sp-band and a much narrower d-band with a higher density of electronic states [20,36–38]. In this section, we will carry out a density-of-states analysis of H, O and OH bonding on Ag, Pt and Ru clusters in order to assess the different roles played by the interaction with the d-band in these two groups of metals.

From a tight-binding analysis, it is known that when a localized energy level, such as an adsorbate orbital, interacts with a wide band of delocalized states, such as the sp band of a metal, the localized orbital is broadened into a Lorentzian projected density-of-states (Fig. 3(a)) [36,37]. This is known as the weak adsorption limit. The OPDOS measures the bonding or antibonding character of the interaction of the localized level with the metal levels, and for the interaction with a wide band of sp states it has the typical bimodal shape as also depicted in Fig. 3(a) [37]. Positive (negative) OPDOS signifies bonding (antibonding) character. On the other hand, when the localized adsorbate level interacts with the more localized d states on the metal, bonding and antibonding orbitals are produced as in a two-level problem, as illustrated in Fig. 3(b). The bonding character of the low energy state shows up as a

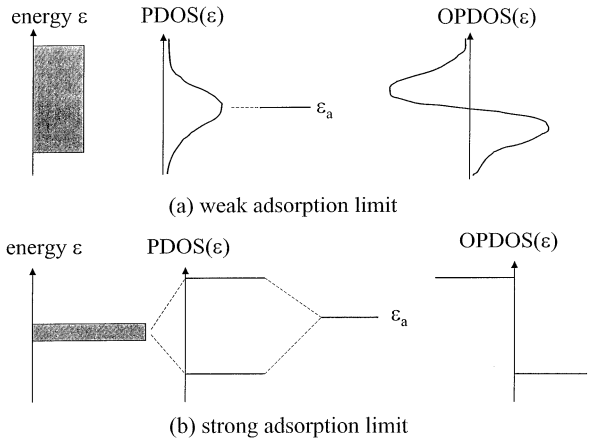

Fig. 3. Interaction of an adsorbate orbital ε_a, with (a) a broad sp-band of metal levels, the weak adsorption limit, and (b) a narrower d-band of metal levels, the strong adsorption limit. Shown are the resulting PDOS and OPDOS of the adsorbate orbital.

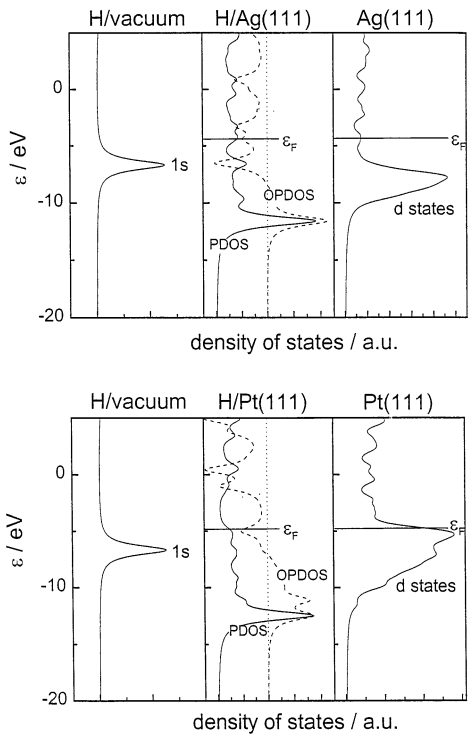

Fig. 4. The hydrogen 1s orbital (left panels) interacting with the metal states (right panels) for Ag and Pt. The middle panels show the resulting 1s PDOS and the 1s-metal d OPDOS. The dashed line in the middle panels gives the zero for the OPDOS.

positive OPDOS peak, whereas the antibonding high-energy state gives rise to a negative OPDOS peak (Fig. 2(b)). This case is also known as the strong adsorption or surface molecule limit.

One may assume, as was done by Norskøv and co-workers [36,20], that the differences in adsorbate bonding among different metals is primarily explained by the difference in interaction with the d band states. The covalent bonding due to the hybridization of the orbitals becomes stronger with a decreasing filling of the d band as this avoids occupying the antibonding resonances of the surface molecule. However, in the extended Hückel approximation, one must also account for the orthogonalization of the orbital wave functions, an effect which lies at the basis of the so-called Pauli repulsion. The orthogonalization energy cost increases with the overlap between the adsorbate state and the metal d states, and this overlap increases down a group and decreases to the right within a series of the periodic table [20]. Hence, one expects a stronger Pauli repulsion moving towards the lower left corner of the periodic table. This competition between the attractive covalent bonding with the d states and the repulsive Pauli contribution can explain quite a few trends in the adsorption energies of simple adsorbates on metals.

Fig. 4 shows the DOS analysis of H adsorption in the hollow site of the Ag(111) and Pt(111) clusters. The left- and right-hand panels of the figure show the density-of-states of the isolated fragments, H and Ag/Pt cluster. The middle panel shows the PDOS of the hydrogen 1s orbital, as well as the OPDOS of the H 1s with the metal d states. The positive and negative OPDOS peaks characteristic for the surface molecule limit are clearly seen for both cases. For Ag, the bonding and antibonding contributions of the interaction with the d states are seen to cancel each other out, because the d band is completely filled. For Pt, the H 1s interaction with the metal d states is of net bonding character as the d band is incompletely filled, and hence more electrons occupy bonding states than antibonding states. Hence, the favorable interaction with the d states makes the H interaction with transition metals stronger than with coinage metals. The trends within the two groups of metals are not so easy to understand with this model. In fact, within the group of the transition metals, the differences are generally quite small and there is no clear trend with the d band filling (see Ref. [36]).

A very similar picture applies to oxygen adsorption, as is illustrated in Fig. 5 for O adsorption on Ag(111) and Ru(0001). It is clearly seen from the OPDOS of the O 2p with the Ag d states that this interaction is essentially nonbonding as both the bonding and antibonding states are completely filled. For Ru, however, this interaction is predominantly bonding, as the main antibonding resonance lies above the Fermi level. The trend among the transition metals can now be easily understood as a consequence of the different d band fillings: with decreasing d band filling, i.e. Pt–Rh–Ru, the antibonding resonances are left unoccupied and hence the overall oxygen interaction becomes stronger. The trend among the coinage metals, i.e. the adsorption energy getting weaker down the row in the periodic table, has been explained by Hammer and Norskøv [20]

as a result of the increasing overlap of the O 2p orbital with the metal d states. In the extended Hückel approximation, this leads to a stronger Pauli repulsion and hence to a weaker overall interaction. The stronger Pauli repulsion can indeed be seen in Table 8 as the equilibrium distance increases from Cu to Ag to Au. This explanation works fine for oxygen adsorption, but apparently fails for H adsorption, for which the Pauli repulsion seems to be less important than for oxygen.

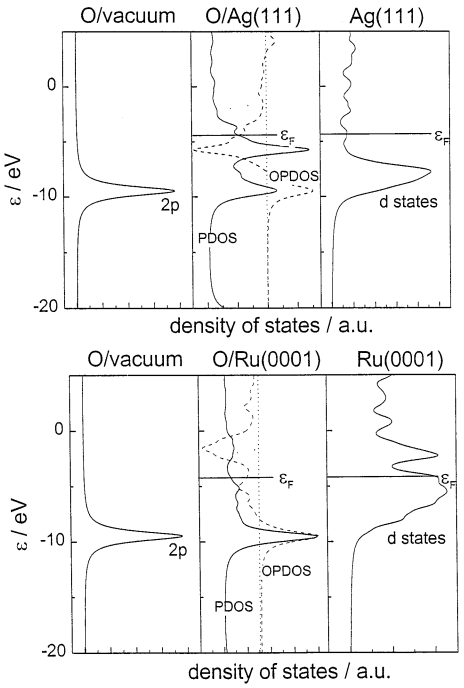

Fig. 5. The oxygen 2p orbital (left panels) interacting with the metal states (right panels) for Ag and Pt. The middle panels show the resulting 2p PDOS and the 2p-metal d OPDOS. The dashed line in the middle panels gives the zero for the OPDOS.

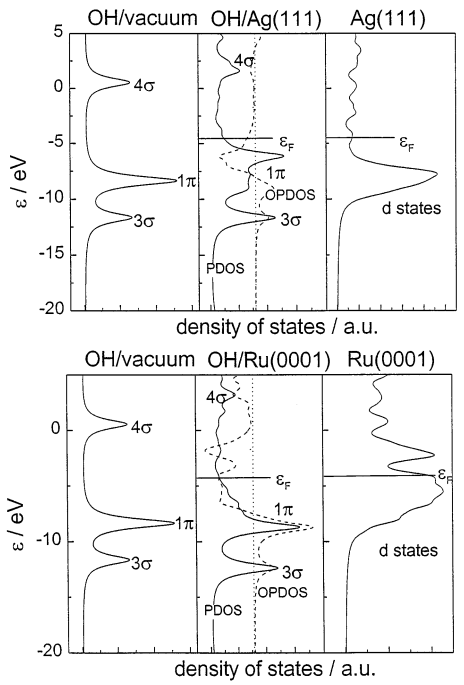

Fig. 6. The hydroxyl 3σ, 1π and 4π orbitals (left panels) interacting with the metal states (right panels) for Ag and Pt. The middle panels show the resulting PDOS and the OPDOS with metal d states. The dashed line in the middle panels gives the zero for the OPDOS.

For OH adsorption, the DOS analyses for the interaction with Ag and Ru are shown in Fig. 6. The main interaction is clearly seen to occur through the OH 1π valence orbital. Because of the lower degeneracy of the OH 1π orbital with respect to the O 2p orbital, and the extra electron density due to the H, the equilibrium bond distance is ca. 0.2–0.3 Å longer than for oxygen. This explains why the interaction with the metal d states is less effective than for oxygen, and that in general the OH bonding to transition metals is not very much stronger than to coinage metals. The trend among the coinage metals may again be explained in a similar fashion as for oxygen, as the equilibrium distance increases from Cu to Au, in agreement with the increasing amount of overlap of the 1π wave function with the metal d states as one moves down the row in the periodic table. In the transition metal group, the trend does not correlate with the amount of d band filling any more, as for oxygen. Pauli repulsion effects will play a role, as the orbital overlap between the OH 1π and the metal d states is expected to be weaker for Rh than for Ru. Hence it follows that for OH chemisorption, less importance should be attached to the covalent bonding contribution [39] because of the lower degeneracy of the OH 1π level with respect to the O 2p level, and because of the increased electron density on the adsorbate with respect to oxygen which pushes the adsorbate away from the surface. To show that this reasoning does indeed give a reasonable description of the OH adsorption trends, we consider the following expression for the adsorption energy, in which the interaction energy with the d band is treated by perturbation theory:

$$\Delta E_b = \Delta E_b^{sp} - 4(1-f)\frac{\beta V_{ad}^2}{|\varepsilon_d - \varepsilon_{1\pi}|} + 4(1+f)\alpha\beta V_{ad}^2 \qquad (4.1)$$

where ΔE_b^{sp} is the contribution to the total adsorption energy due to the interaction with the sp electrons, f is the fractional filling of the d band (taken equal to their idealized values, 0.7, 0.8 and 0.9 for Ru, Rh and Pt, respectively, and 1 for Cu, Ag, and Au), V_{ad}^2 is the (relative) adsorbate 1π-metal d coupling matrix element (values taken from fig. 18 in Ref. [20]), ε_d is the center of the d band (values taken from fig. 18 in Ref. [20]), $\varepsilon_{1\pi}$ is the 1π energy level close to the surface, β is the ratio of the real and relative coupling matrix elements, and α the ratio of the overlap matrix element and the coupling matrix element. The second term on the right-hand side of Eq. (4.1) is the hybridization energy gain

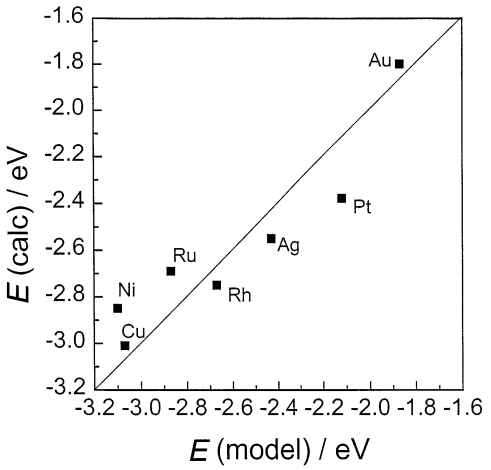

Fig. 7. The DFT-calculated OH adsorption energies vs. the model-calculated adsorption energies from Eq. (4.1). $E_0 = -3.58$ eV, $\varepsilon_{1\pi} = -5$ eV, $\beta = 0.75$, $\alpha = 0.085$.

(covalent attraction), whereas the third term is the orthogonalization energy cost (Pauli repulsion). The perturbation theory expression is usually not accurate from the purely numerical point-of-view, but works well when aiming at qualitative trends. Any numerical errors may be considered to be incorporated in the quantities ΔE_b^{sp}, α and β, which we take as independent of the metal. Fig. 7 shows the correlation between the DFT-calculated and model-calculated adsorption energies. We have included in Table 9 and in the figure the OH adsorption energy on Ni(111), as the perturbation-theory expression suggests that Ni is an interesting case for comparison with Ru. According to Eq. (4.1), OH is expected to interact more strongly with Ni than with Ru, whereas exactly the opposite holds for O, according to the results of Hammer and Nørskov [20]. This is due to the fact that although the d band filling of Ni is higher than that of Ru (which favors O adsorption on Ru), the Pauli repulsion on Ni is much weaker than on Ru and this favors OH adsorption. This is indeed found from the DFT calculations. Considering the simplicity of Eq. (4.1), the agreement shown in Fig. 7 is quite satisfactory and supports our view that the covalent contribution for hydroxyl adsorption is less important than for oxygen.

5. Conclusions

In this paper, we have studied the adsorption characteristics of the water dissociation products H, O, and OH on a variety of metal surfaces by quantum chemical DFT calculations. These adsorbates are of importance in many electrochemically and heterogeneously catalyzed reactions. We summarize our main findings.

- On all metals, we find that O and OH prefer the three-fold hollow sites to the on-top site. In contrast, no uniquely preferred adsorption site is found for H. Especially for transition metals, we find that the energetic difference between H adsorbed at on-top and three-fold hollow sites is small. It seems that at finite coverages lateral interactions will be very important in choosing the preferred adsorption site, an issue that clearly deserves more detailed attention in the future.
- From analyzing the Mulliken and Hirshfeld adsorbate charges, dipole moment curves and the field dependence of the chemisorption bond, it is found that H forms an essentially covalent bond with the Ag(111) surface, whereas O and OH form a largely ionic bond. The H–Ag cluster bond is not strongly electric field dependent, whereas both O and OH are pulled towards the surface when a positive field (more positive electrode potential) is applied across the cluster. Both adsorbates become less negatively charged when a positive field exists; the 'intrinsic' O adsorption energy becomes less negative with a more positive field, though not by a large amount, whereas the H and OH adsorption energies do not show a significant field dependence in our calculations. The fact that bonding energies are not very much dependent on the applied field agrees with results of Siegbahn and Wahlgren [12], who found that shifting the Fermi level by 7 eV, by adding and removing electrons from a cluster, changed the hydrogen chemisorption energy by less than 0.1 eV. Hence, the main reason why electrochemical reactions, even those involving adsorbed species, are potential dependent is because the electrons are stored at or taken from a different Fermi level. Since these electrons are, in contrast to the metal | vacuum situation, detected in the external circuit, this results in a detectable change in the overall reaction energy.
- Atomic hydrogen binds more strongly to transition metals than to the noble coinage metals on account of the more favorable interaction with the partially filled d band of the transition metals. The trend among the transition metals does not seem to correlate very strongly with the amount of d band filling. The calculated adsorption energies for the transition metals, ca. -2.60 eV, agree very well with the existing experimental estimates.
- Atomic oxygen binds more strongly to transition metals than to the noble coinage metals again due to the role played by the partially filled d band of the transition metals. For transition metals, the chemisorption bond gets stronger with a lower d band filling. For the coinage metals, the chemisorption bond gets stronger with a smaller overlap of the oxygen 2p state with the metal d band states, leading to a smaller Pauli repulsion. The calculated adsorp-

tion energies agree quite well with slab calculations (which assume finite coverages, and hence include lateral interactions) and experimental estimates.

- The trends in the bonding of molecular hydroxyl can be understood using a similar reasoning as for atomic oxygen, if one accounts for the weaker covalent interaction with the d states due to the lower degeneracy of the OH 1π level in comparison with the O 2p level, and the presence of the hydrogen which pulls the adsorbate away from the surface. As a result, the bonding to the transition metals is not systematically stronger than to the coinage metals, and the role of Pauli repulsion becomes more important due to the increased electron density on the adsorbate.
- We believe our results should be reasonably accurate as zero-coverage binding energies for adsorbates at the metal | vacuum interface. For adsorbates whose main bonding interaction is covalent, we expect the binding energies at the metal | vacuum and metal | liquid interfaces to be comparable. This is corroborated by Jerkiewicz's results [35] that the experimental H adsorption energy on transition metal electrodes is very similar to that on the same metals in vacuum. However, for ionic adsorbates one expects a much stronger interaction with the solvent, and the results will not be directly applicable to the metal | liquid interface. This is neatly illustrated by the adsorption of halides on metal surfaces, where the calculated trends are opposite to those observed in the electrochemical situation [38].

Acknowledgements

M.T.M.K. acknowledges a grant from the Royal Netherlands Academy of Arts and Sciences (KNAW).

References

[1] D.L. Price, J.W. Halley, J. Chem. Phys. 102 (1995) 6603.
[2] J.W. Halley, A. Mazzolo, Y. Zhou, D. Price, J. Electroanal. Chem. 450 (1998) 273.
[3] C.P. Ursenbach, A. Calhoun, G.A. Voth, J. Chem. Phys. 106 (1997) 2811.
[4] A. Klesing, D. Labrenz, R.A. van Santen, J. Chem. Soc., Faraday Trans. 94 (1998) 3229.
[5] E. Spohr, J. Phys. Chem. 93 (1989) 6171.
[6] I. Benjamin, in: J.O'M. Bockris, B.E. Conway, R.E. White (Eds.), Modern Aspects of Electrochemistry, vol. 31, Plenum Press, New York, 1997, p. 115.
[7] R.R. Nazmutdinov, M.S. Shapnik, Electrochim. Acta 41 (1996) 2253.
[8] An. Kuznetsov, J. Reinhold, W. Lorenz, Electrochim. Acta 29 (1984) 801.
[9] G.te Velde, E.J. Baerends, Phys. Rev. B 44 (1991) 7888.
[10] M.C. Payne, M.P. Teter, D.C. Allen, T.A. Arias, J.D. Joannopoulos, Rev. Mod. Phys. 64 (1992) 1045.
[11] G.te Velde, E.J. Baerends, Chem. Phys. 177 (1993) 399.
[12] P.E.M. Siegbahn, U. Wahlgren, in: E. Shustorovich (Ed.), Metal-Surface Reaction Energetics, VCH, New York, 1991, p. 1.
[13] R.A. van Santen, M. Neurock, Catal. Rev.-Sci. Eng. 37 (1995) 557.
[14] H. Yang, J.L. Whitten, Surf. Sci. 223 (1989) 131.
[15] A. Fahmi, R.A. van Santen, Z. Phys. Chem. 197 (1997) 203.
[16] Amsterdam Density Functional Package, ADF 2.3.0, Department of Theoretical Chemistry, Vrije Universiteit, Amsterdam, 1997.
[17] E.J. Baerends, D.E. Ellis, P. Ros, Chem. Phys. 2 (1973) 41.
[18] G.te Velde, E.J. Baerends, J. Comput. Phys. 99 (1992) 84.
[19] D.R. Lide (Ed.), Handbook of Physics and Chemistry, 71st ed., CRC Press, Boca Raton, 1990.
[20] B. Hammer, J.K. Nørskov, in: R.M. Lambert, G. Pacchioni (Eds.), Chemisorption and Reactivity on Supported Clusters and Thin Films, NATO ASI Series, vol. 331, Kluwer Academic Publishers, Dordrecht, 1997, p. 285.
[21] F. Jensen, Introduction to Computational Chemistry, Wiley, Chicester, 1999.
[22] S.H. Vosko, L. Will, M. Nusair, Can. J. Phys. 58 (1980) 1200.
[23] A.D. Becke, Phys. Rev. A 38 (1988) 3098.
[24] A.D. Becke, ACS Symp. Ser. 394 (1989) 165.
[25] J.P. Perdew, Phys. Rev. B 33 (1986) 8822.
[26] F.L. Hirshfeld, Theoret. Chim. Acta 44 (1977) 129.
[27] R. Hoffmann, Solids and Surfaces: a Chemists View of Bonding in Extended Structures, VCH, New York, 1988.
[28] I. Panas, J. Schüle, P. Siegbahn, U. Wahlgren, Chem. Phys. Lett. 149 (1988) 265.
[29] P.E.M. Siegbahn, U. Wahlgren, Int. J. Quant. Chem. 42 (1992) 1149.
[30] K. Hermann, M. Witko, L.G.M. Petterson, P. Siegbahn, J. Chem. Phys. 99 (1993) 610.
[31] P.S. Bagus, G. Pacchioni, M.R. Philpott, J. Chem. Phys. 90 (1989) 4287.
[32] F.M. Bickelhaupt, N.M.M. Nibbering, E.M. van Wezenbeek, E.J. Baerends, J. Phys. Chem. 96 (1992) 4864.
[33] J.B. Benzinger, in: E. Shustorovich (Ed.), Metal-Surface Reaction Energetics, VCH, New York, 1991, p. 53.
[34] O.M. Løvvik, R.A. Olsen, Phys. Rev. B 58 (1998) 10890.
[35] G. Jerkiewicz, Prog. Surf. Sci. 57 (1998) 137.
[36] S. Holloway, B.I. Lundqvist. J.K. Nørskov, Proceedings of the International Congress on Catalysis, vol. 4, Berlin, 1984, p. 85.
[37] R.A. van Santen, Theoretical Heterogeneous Catalysis, World Scientific, Singapore, 1991.
[38] M.T.M. Koper, R.A. van Santen, Surf. Sci. 422 (1999) 118.
[39] M. Chen, S.P. Bates, R.A. van Santen, C.M. Friend, J. Phys. Chem. B 101 (1997) 10051.